Reconstruction of the Hadronic Calorimeter Energy using the shower topology weighting technique

R. Garabík, P. Holík G. Krajčovič, P. Šťavina, S. Tokár, T. Ženiš
Dep. of Nuclear Physics
Comenius University
Mlynská dolina F1
Bratislava
SLOVAKIA

Abstract

A method for calorimeter energy reconstruction using information about hadronic shower topology parameters has been developed and used to reconstruct the data from September 1996 and May 1995 stand alone testbeam runs.

1 Introduction

One of the main problems in hadron calorimetry is to cope with non-compensation effect. This effect is caused by different response of calorimeter to photons and electrons on one side and hadrons on the other side. The fact that share of π_0 energy in hadronic shower is increasing with the incident particle energy has very undesirable consequences. The first of all it leads to non linear dependence of the calorimetric response from the incident hadron energy. Except of that the ratio of π_0 fluctuates a lot and it leads to deterioration of calorimeter energy resolution. To cope with this problem one needs to suppress the signal fluctuations originating in the fluctuations of π_0 energy. with π_0. One approach was presented by H1 collaboration [1]. In our work we are presenting the method which is based on employment of some internal shower parameters which can distinguish between the events with different share of π_0 energy. Essentially we can say that in the transverse dimensions of showers there is coded also an information on the share of π_0 energy. The events with the high share of π_0 in shower are narrower and have a bigger response if compared with those of low π_0 share.

In our analysis we have used the experimental data taken in the test beam runs of the ATLAS calorimeter prototype which were carried out in May 1995 and September 1996. The tested calorimeter prototypes are quit well segmented in longitudinal as well as in transverse directions [2, 3] therefore can be used for distinguishing of different hadronic shower topologies.

2 R_t weighting technique

The presented method is based on the idea that it is possible to find a parameter sensitive to share of π_0 energy in hadronic shower and use

it as a calibration parameter on event-by-event basis. The essence of the calibration is in determining of the value of the π_0 sensitive parameter for each event and to employ the found dependence of reconstructed signal on the calibration parameter as a calibration curve. To achieve this goal we need:

- to define the calibration parameter
- to find the corresponding calibration curve

2.1 Shower radius

The simplest way of finding the parameters sensitive to the share of π^0 energy is to use the fact that the events with a high share of π^0 are narrow and have a big signal. There are different possibilities for definition of such parameters, we have looked at the following ones:

$$r_T^{(1)} = \frac{\sum_{i=1}^{N_{cell}} r_i \cdot S_i}{\sum_{i=1}^{N_{cell}} S_i} \tag{1}$$

$$r_T^{(2)} = E_{inc} \cdot \frac{\sum_{i=1}^{N_{cell}} r_i \cdot S_i}{\left(\sum_{i=1}^{N_{cell}} S_i\right)^2} = r_T^{(1)} \cdot \frac{E_{inc}}{E_{rec}} \tag{2}$$

$$r_T^{(3)} = \begin{cases} \frac{\sum_{i=1}^{N_{cell}} r_i \cdot S_i}{\sum_{i=1}^{N_{cell}} S_i} & r_i > 10cm \\ 0 & r_i < 10cm \end{cases} \tag{3}$$

$$r_T^{(4)} = \sqrt{\frac{\sum_{i=1}^{N_{cell}} r_i^2 \cdot S_i}{\sum_{i=1}^{N_{cell}} S_i}} \tag{4}$$

$$r_T^{(5)} = \frac{\sum_{i=1}^{N_{cell}} r_i \cdot S_i \cdot \left(1 - e^{-r_i/D}\right)}{\sum_{i=1}^{N_{cell}} S_i} \tag{5}$$

where

- $S_i = S_i^{(1)} + S_i^{(1)}$ is the signal from i^{th} cell (1^{st} PMT and 2^{nd} PMT)
- r_i is the distance from the centre of i^{th} cell to the shower axis
- E_{inc} (E_{rec}) is the incident (reconstructed) energy
- N_{cell} is the number of cell involved
- D is a characteristic shower radius

2.2 Event by event calibration

Application of the above mentioned technique to experimental data consists in reconstructing of both the energy (E_{rec}) and shower transverse parameter (r_T) event by event followed by finding of a dependence of E_{rec} on shower transverse parameter. We assume that the mean value of E_{rec} taken at given r_T depends on r_T as

$$\bar{E}_{rec} = E_{inc} \cdot f(r_T) \tag{6}$$

The presented method is suggested in order to remove or reduce the energy fluctuations which originate in the dependence of calorimeter signal on calibration parameter - the shower radius in our case. The energy fluctuations can be expressed as

$$\sigma^2_{E_{rec}} = \sigma^2_{r_T} + \sigma^2_{nom} \tag{7}$$

where σ^2_{nom} is a non-reducible part of dispersion, caused by sampling fluctuations, electronics and detector noise etc, and the term $\sigma^2_{r_T}$ represents the fluctuations stemming from the dependence of calorimeter signal on shower radius. The $\sigma^2_{r_T}$ is, in principle, removable by the calibration procedure consisting in correction of the reconstructed energy by means of

$$E_{cor} = \frac{E_{rec}}{f(r_i)} \tag{8}$$

where $f(r_i)$ is a calibration curve. In an optimal case the $\sigma^2_{r_T}$ part of the fluctuations should be removed by the calibration procedure. In that case for the dispersion of E_{cor} we get:

$$\sigma^2_{E_{cor}} = \sigma^2_{E_{nom}} \tag{9}$$

2.3 Choice of the correction function

We start with a natural relation between incident energy (E_{inc}) and mean signal ($\bar{S}$) in calorimeter.

$$\bar{S} = h(E_{inc} - E_{\pi^0}) + e \cdot E_{\pi^0} \tag{10}$$

which can be expressed as

$$\bar{S}(E_{inc}) = h \cdot E_{inc} \cdot \left(1 + \left(\frac{e}{h} - 1\right) \cdot f_{\pi^0}(E_{inc})\right) \tag{11}$$

where e and h are the energy-to-signal conversion factors for pure electromagnetic showers and hadrons, respectively, E_{π^0} is the π^0 energy contained in hadronic shower, and $f_{\pi^0}(E_{inc})$ is the share of π^0 energy in hadronic shower energy.

In our approach we have generalised the function f_{π^0} by including the shower transverse radius as an additional parameter, and obtained the following expression for the mean signal:

$$\bar{S}(E_{inc}, r_T) = h \cdot E_{inc} \cdot \left(1 + \left(\frac{e}{h} - 1\right) \cdot F_{\pi^0}(E_{inc}, r_T)\right) \tag{12}$$

We have factorized the function F_{π^0} as follows:

$$F_{\pi^0}(E_{inc}, r_T) = f_{\pi^0}(E_{inc}) \cdot F(r_T) \tag{13}$$

At first we have chosen $F(r_T)$ in the following form:

$$F(r_T) = c \cdot e^{-\lambda \cdot r_T} \tag{14}$$

In this case the pure hadronic energy corresponds to $r_T \to \infty$, and pure electromagnetic energy to $r_T \to 0$. A natural condition can be imposed on $\bar{S}(E_{inc}, r_T)$:

$$\bar{S}(E_{inc}) = \int \bar{S}(E_{inc}, r_T) \cdot w(r_T) \cdot dr_T \tag{15}$$

Where $w(r_T)$ is distribution of events in shower radius r_T.

This condition entails in the following restriction on the parameter c of $F(r_T)$:

$$f_\pi \cdot c = 1 \tag{16}$$

Other and more realistic expression for $F(r_T)$ can be chosen in the form:

$$F(r_T) = c \cdot \left(\frac{R_m - r_T}{R_m - R_0}\right)^\alpha \tag{17}$$

R_0, R_m are the parameters characterizing shower topology with respect to the share of hadronic energy in it. R_m represents a shower radius at which the function $F(r_T)$ reaches the saturation corresponding to the pure hadronic showers (absence of π_0). On the other hand, R_0 is a characteristic radius corresponding to the pure electromagnetic showers. In principle these saturation radii, as well as their dependece on tilt angle, incident point, etc., can be determined by Monte Carlo simulations.

The parameters R_0, R_m should not be strongly dependent on incident energy, however one can anticipate that R_0 would show some dependence on energy, because of finite granularity of the calorimeter. This circumstance could play more significant role especially for the data taken by the 5 modules prototype in May 1995 test beam.

For the pure hadronic energy we have $\bar{S}(E_{inc}, r_T \to R_m) \to h \cdot E_{inc}$, and for the electromagnetic one $\bar{S}(E_{inc}, r_T \to R_0) \to e \cdot E_{inc}$. These limits lead again to the condition (16). The advantage of the parametrisation (17) over that of (14) is that the former gives more natural limits for the pure electromagnetic and hadronic energy. The final form of the correction function, which was employed in our analysis is:

$$e^{-1} \cdot \bar{S}(E_{inc}, r_T) = h' \cdot E_{inc} \cdot \left(1 + \left(\frac{1}{h'} - 1\right) \cdot \left(\frac{R_m - r_T}{R_m - R_0}\right)^\alpha\right) \tag{18}$$

where $h' = h/e$ and α are the only parameters describing the calorimeter for given energy.

The calibration of the calorimeter was carried out with the electron beams, therefore we have to multiply the reconstructed energy by e^{-1} to have the signal in the calorimeter expressed in GeV.

There are also events with non negligible energy leakage from the calorimeter. Such events are characterised by lower total energy, and it is desirable to use some sort of correction for such events, to decrease their overall negative effect on reconstructed energy. For the time being we have taken into account only the events with a noticeable signal in the first sampling. The chosen threshold is 5% of the total energy.

The sense of this prerequisite is to eliminate the events starting late, and thereby having leakage, and allows us to concentrate on the method without disturbing effects. The requirement to have a non-zero energy release in the first sampling is not very restrictive from the physical point of view. It only removes the showers starting late, but it has no impact on other physical properties, like the amount of π^0, etc. This restriction means that we have to do with the events of the same class from the calorimeter point of view and it simplifies the data analysis. The events starting late can be treated separately including also the information from other detectors, like muon counters.

3 Analysis of the experimental data

The above mentioned weighting technique of energy reconstruction has been applied on the experimental data taken in the test beam runs in the years 1995 and 1996. The experimental setups used in these tests are shown in Fig. 1 and 2. The detailed description of the setups and the run conditions has been given elsewhere [2, 3, 4]. In the above mentioned test beam runs the calorimeter prototypes responses to different incident particles (pions, electrons and muons) in the energy range from 10 GeV to 300 GeV and different incident angles were measured.

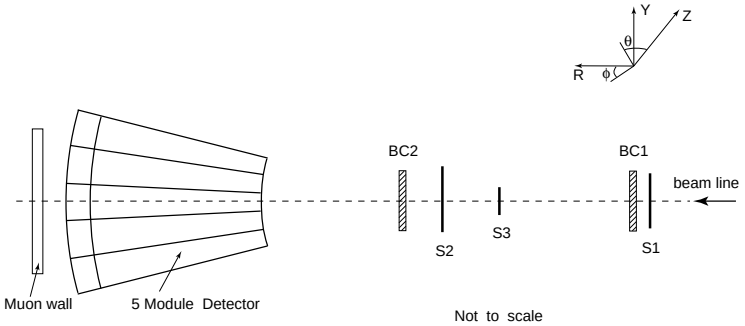

Figure 1: Setup used in May 1995 testbeam

3.1 The 1995 test beam experiment

The results of the 1995 test beam data analysis are presented in Figs. 6, 3, 8, 9 and Table 1. In the analysis the test beam data from the above mentioned pion beam energy range and incident angle of 10° were taken into account. In Fig. 3 dependences of the reconstructed signal $\bar{S}(E_{inc}, r_T)$

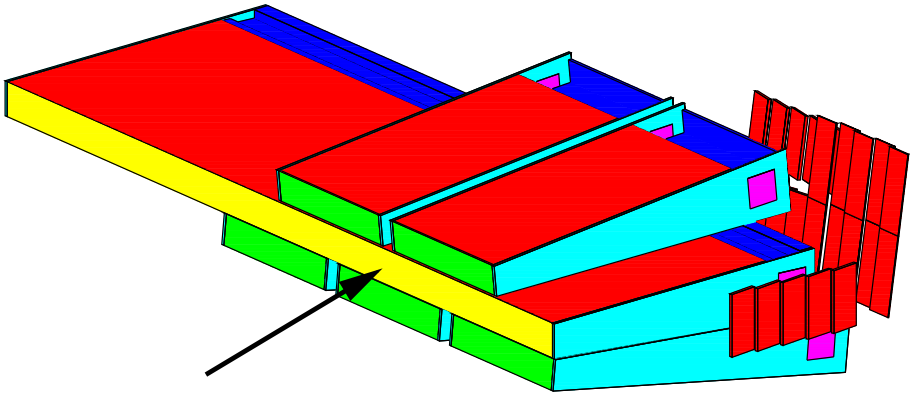

Figure 2: Setup used in Module 0 July 1996 testbeam

as a function of shower radius are shown for different incident energies. For convenience instead of the mean signal ($\bar{S}$) its ratio to incident energy ($\bar{S}/E_{inc}$) is depicted as a function of r_T. The r_T-dependences have been fitted using the function (18). At the fits only the parameter α was free. The parameter h was found as a ratio $\bar{S}/E_{inc}$ using the events with high r_T. Averaging this ratio for the all incident energies we found the value of $h = 4.82$ using the events which show saturation of this ratio with respect to the dependence $E_{rec}/E_{inc} = f(r_T)$, as is shown in Figs. 4, 5. The value of e/h was fixed at 1.32 [5]. The dependence of the parameter α on incident energy is shown in Fig. 6. The pure hadronic energy saturation radius R_m has been taken to be the same for all incident energies (15 cm), while the pure electromagnetic energy one (R_0) has been fitted by a power function as is shown in Fig. 7. Fixing all parameters in (18), one can use this equation for finding of the real energy by expressing E_{inc} through $\bar{S}$ and the correction function. The linearity and energy resolution for the corrected energy are shown in Figs. 8 and 9, respectively. From the figures we see that the linearity is at a level of 1% and the resolution is better the in the case of the benchmark[1] approach.

3.2 The 1996 test beam experiment

The 1996 test beam data were analysed in the same manner as the data of the 1995 test beam but for two incident particle pseudorapidities ($\eta = -0.25, -0.45$). The results of analysis are presented in the following figures and tables. In Fig. 10 the dependences of reconstructed signal ($\bar{S}/E_{inc}$) as a function of shower radius are shown for different incident energies at the pseudorapidity $\eta = -0.25$ and the same dependences for $\eta = -0.45$ are shown in Fig. 11. These dependences have been fitted using the function (18). The dependence of α on incident energy is shown in Fig. 12 for $\eta = -0.25$ and in Fig. 13 for $\eta = -0.45$. As in the case of the 1995 data the corrected energies were found. The linearity and

[1] by *benchmark* we understand reconstruction of raw, uncorrected energy

energy resolution for the corrected energy for $\eta = -0.25$ are shown in Figs. 14. From the figures we see that the linearity is at a level of 1% and the resolution is better the in the case of the benchmark approach.

There are however some potential problems. First of all the parameter h' should be equal to h/e ($= \frac{1}{e/h}$) which is a constant known from other measurements. In fact, one can use the values of parameter P_1 from tables 2 and 5 to do an independent estimation of e/h value. The average value computed from our results is $e/h = 1.31 \pm 0.05$ for Module 0, which is in a good agreement with [5, 6, 7].

However, it would not be a surprise if h' showed some week dependence on incident energy. The reason is that h' we get as a limit for the small shower radius and taking into account the calorimeter cell dimensions one can expect some systematics in definition of the shower radius. On the other hand for the parameter α, we expect to have an explicit dependency on incident energy.

Indeed, as we can see in Fig. 13, parameter α can be reasonably fitted with exponential function, introducing into the method two energy independent parameters [8].

4 Conclusion

The 1995 and 1996 standalone test beam data have been analyzed with the proposed r_T weighting technique. The application of this technique leads to an improvement of the calorimeter energy resolution if compared with bench mark one and gives a good linearity, at a level of 1%, for the both calorimeter prototypes.

The method contains a small number of parameters which have a clear physical interpretation. In the general form the method contains 6 energy independent parameters.

Two of the parameters, namely the conversion factor e and ratio e/h can be found independently using other analysis techniques.

The saturation radii R_0 and R_m are hadronic shower characteristics and can be determined, including their dependence on incident point, angle of the beam etc., by Monte Carlo simulation.

E_{inc}	$\eta_{notcorr}$	$\eta^{(1)}_{corr}$	linearity	α
10.	21.1	19.6	0.905	3.185
20.	13.5	12.4	1.023	2.256
50.	9.3	8.8	0.990	2.413
100.	6.9	6.4	1.003	2.496
150.	6.6	6.0	1.021	2.784
180.	5.8	5.5	0.993	1.943
200.	6.0	5.3	1.001	2.057
300.	5.4	4.9	0.996	1.637

Table 1: Comparison of corrected and not corrected resolution, May 1995 data.

References

[1] M. P. Casado, M. Cavalli-Sforza, *H1-inspired analysis of the 1994 combined test of the Liquid Argon and Tilecal calorimeter prototypes*, ATLAS Internal Note, ATL-TILECAL-NO-96-075

[2] Tile Calorimeter TDR, 1996, CERN.

[3] B. Di Girolamo, *An overwiev of the ATLAS TILECAL hadronic calorimeter*, ATLAS Internal Note, ATL-TILECAL-NO-96-085

[4] Z. Ajaltouni, et al., *Response of the ATLAS Tile calorimeter prototype to muons*, Nucl. Instr. and Meth. in Phys. Res. A388 (1997) 64-78.

[5] J. A. Budagov, et al., *Electron Response and e/h Ratio of ATLAS Iron-Scintillator Hadron Prototype Calorimeter with Longitudinal Tile configuration*, ATLAS Internal Note, ATL-TILECAL-NO-96-072

[6] Y. A. Kulchitsky, V. B. Vinogradov, *Non-compensation of the ATLAS Barrel Tile Hadron Module-0 Calorimeter*, ATLAS Internal Note, ATL-TILECAL-NO-99-021

[7] I. Efthymiopoulos, *Comparison between the ATLAS/TileCal hadron barrel calorimeter prototype test beam data and Hadronic Simulation packages*, ATLAS Internal Note, ATL-TILECAL-NO-96-092

[8] I. Efthymiopoulos, *ATLAS BAREL HADRON CALORIMETER THE MODULE 0 EXPERIENCE*, ATLAS Internal Note, ATL-TILECAL-NO-98-141

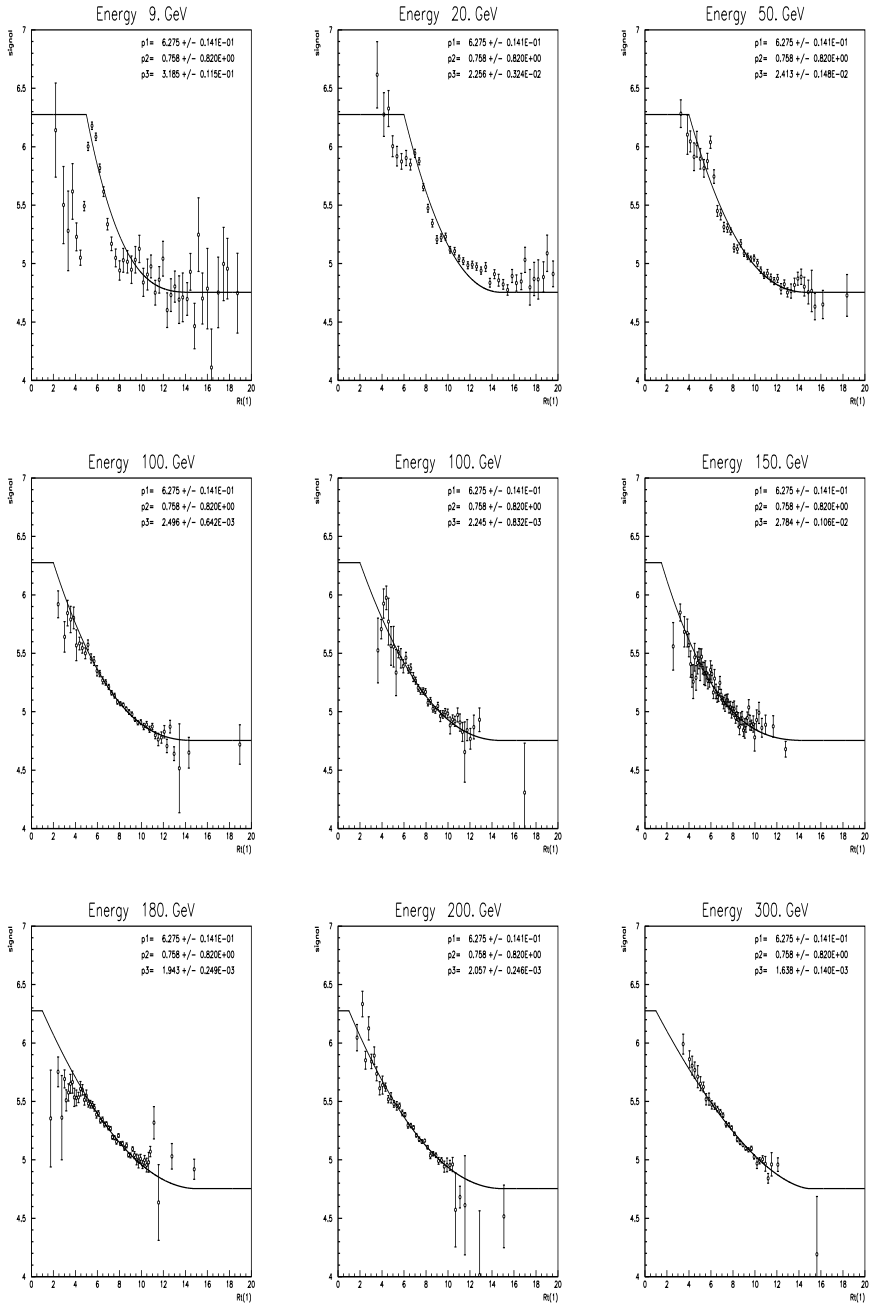

Figure 3: Dependences of the reconstructed energy vs. shower radius r_T for different incident energies, May 1995 data.

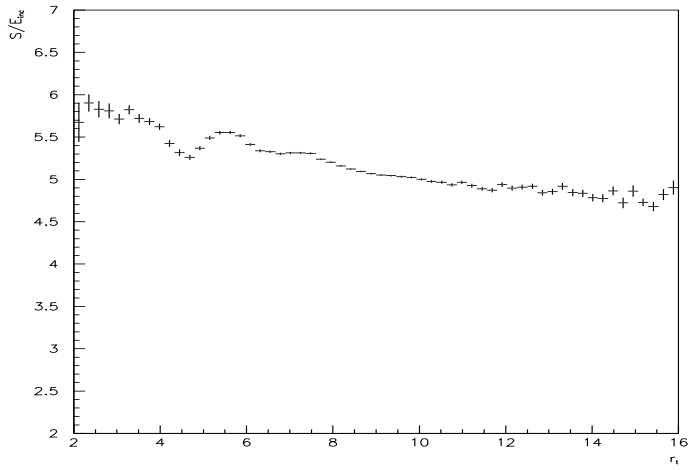

Figure 4: Dependence of Signal/Energy ratio vs. r_T, 1995 test beam data

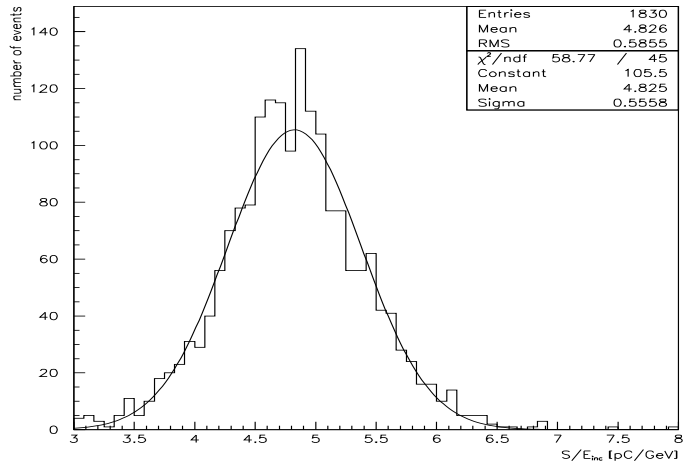

Figure 5: Signal/Energy ratio, 1995 test beam data.

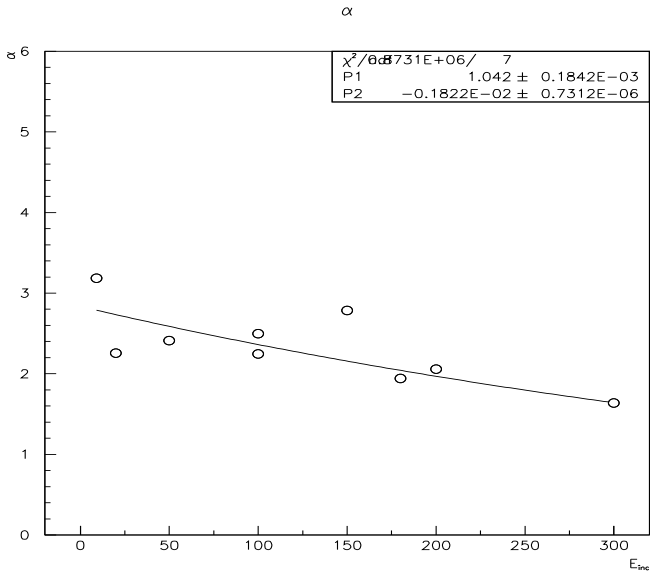

Figure 6: Dependence of α on incident energy E_{inc}, May 1995 data.

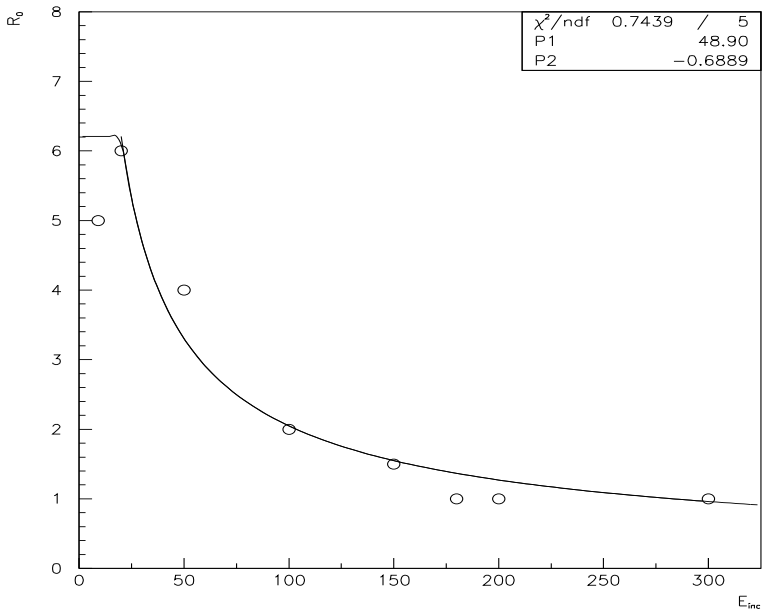

Figure 7: Dependence of R_0 on incident energy E_{inc}, May 1995 data, fitted by power function $r_0 = P_1 \cdot \left(\frac{E}{1\ GeV}\right)^{P_2}$

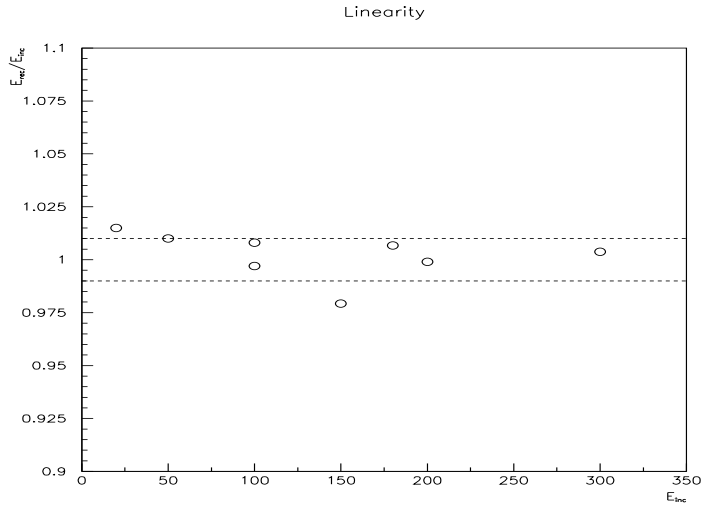

Figure 8: The linearity for the corrected energies, $P_1 = 6.5$, $P_2 = 0.75$, the 1995 test beam data).

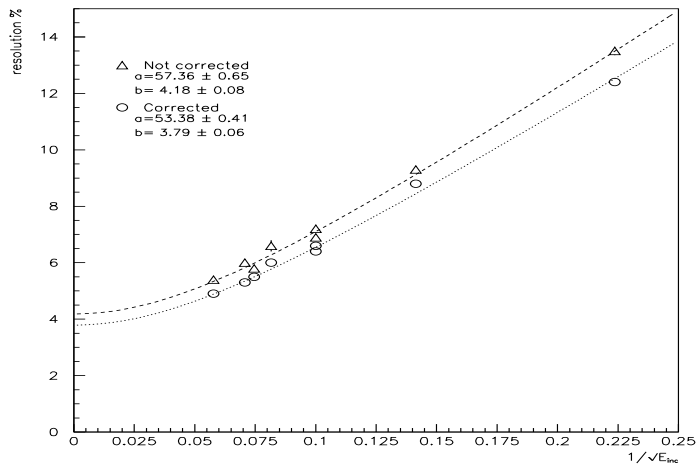

Figure 9: The energy resolution for the corrected energies, $P_1 = 6.5$, $P_2 = 0.75$, the 1995 test beam data).

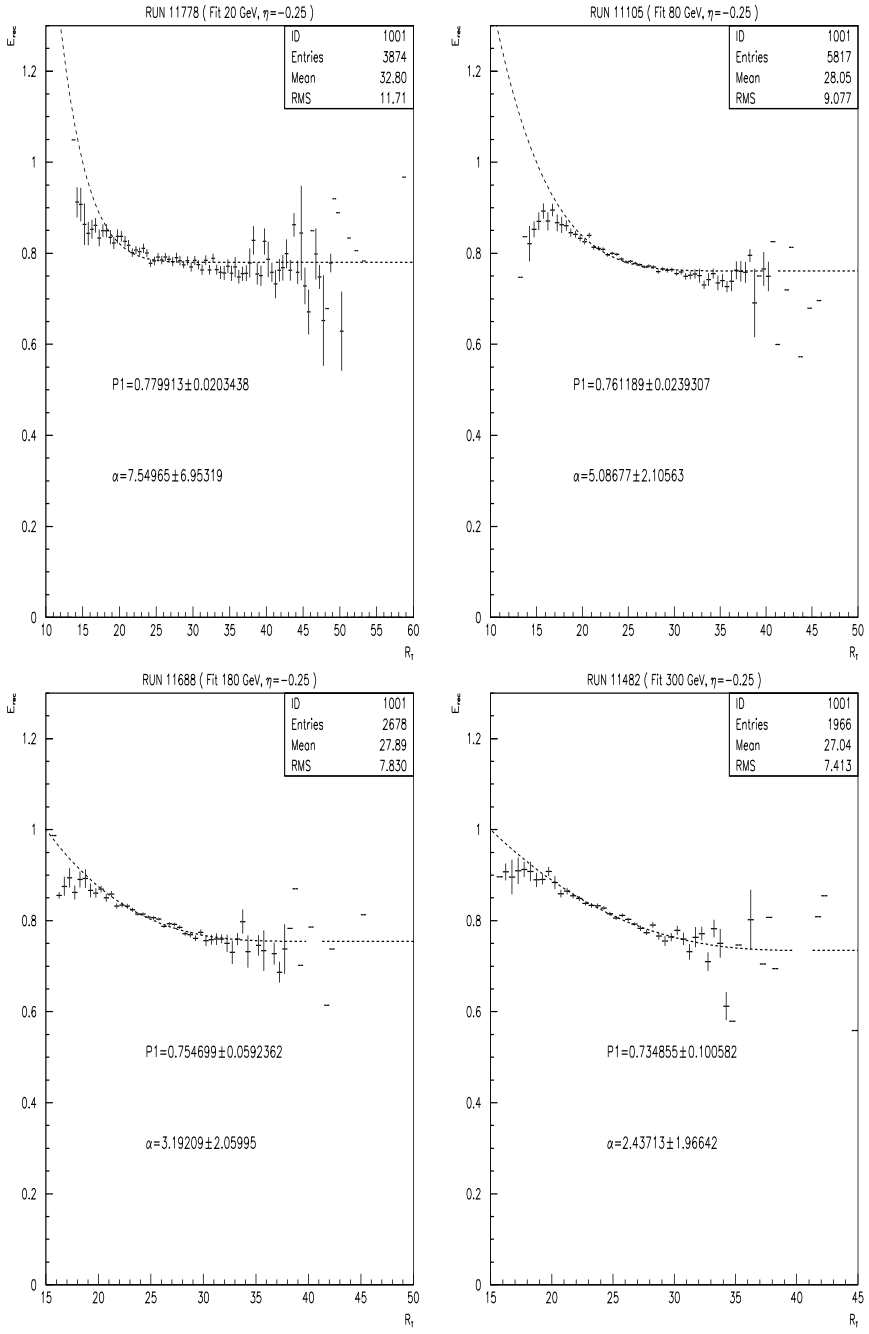

Figure 10: Dependence of the reconstructed energy vs. the shower radius r_T for $\eta = -0.25$ and the incident energies 20, 80, 180 and 300 GeV, the 1996 test beam data.

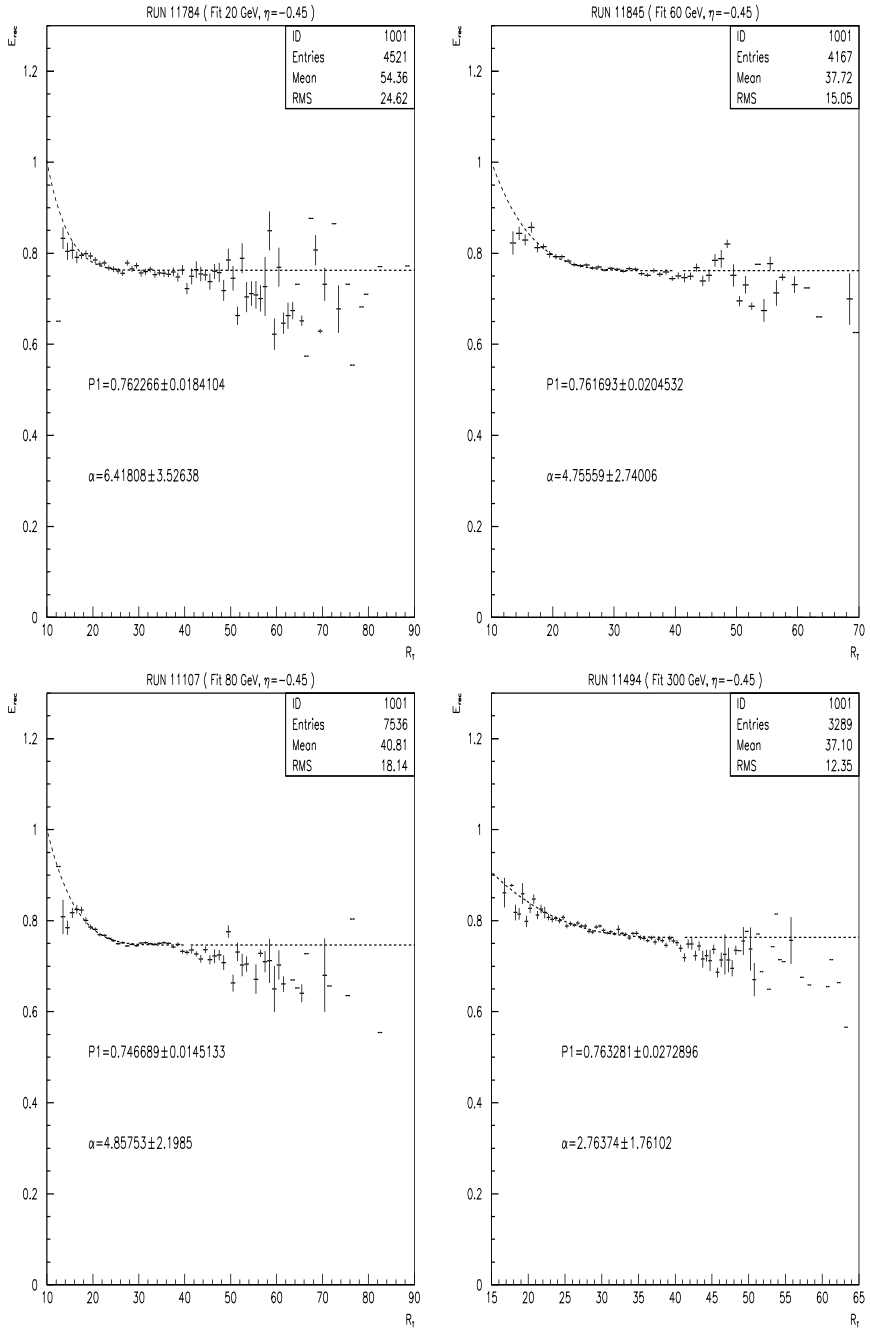

Figure 11: Dependence of the reconstructed energy vs. the shower radius r_T for $\eta = -0.45$ and the incident energies 20, 60, 80 and 300 GeV, the 1996 test beam data.

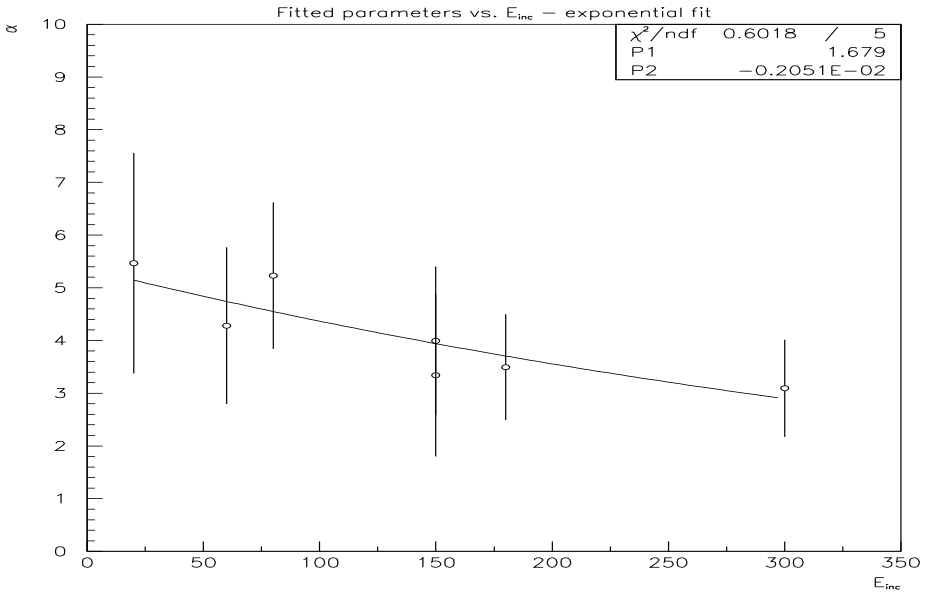

Figure 12: Dependence of the parameter α on incident energy, $P_1 = 0.762$, $\eta = -0.25$, the 1996 teat beam data.

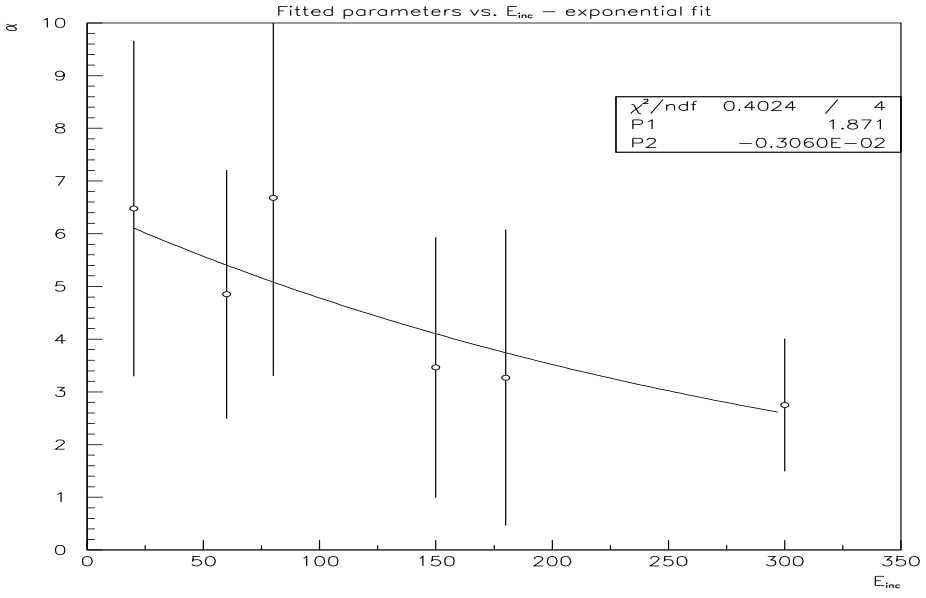

Figure 13: Dependence of the parameter α on incident energy, $P_1 = 0.762$, $\eta = -0.45$, the 1996 teat beam data.

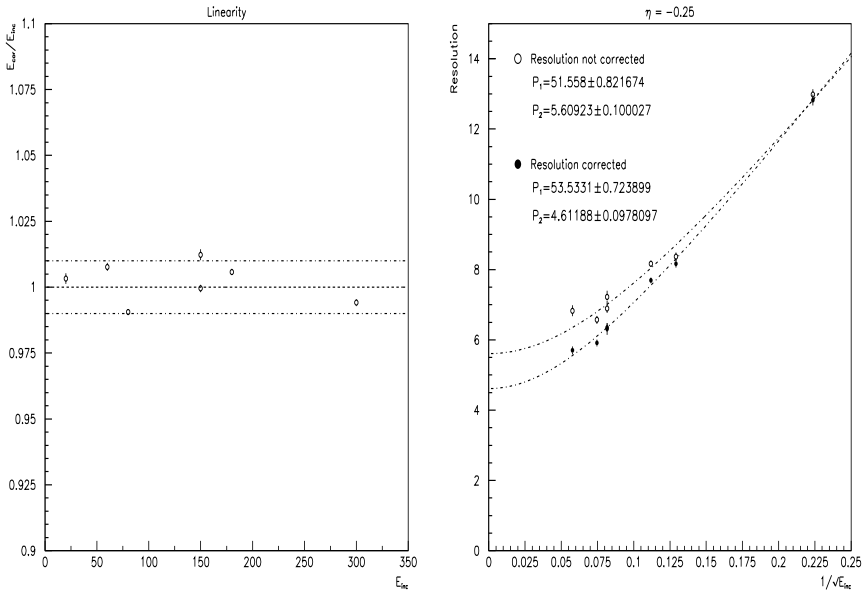

Figure 14: Linearity and resolution of reconstructed energy for global fit, η = -0.25, the 1996 test beam data

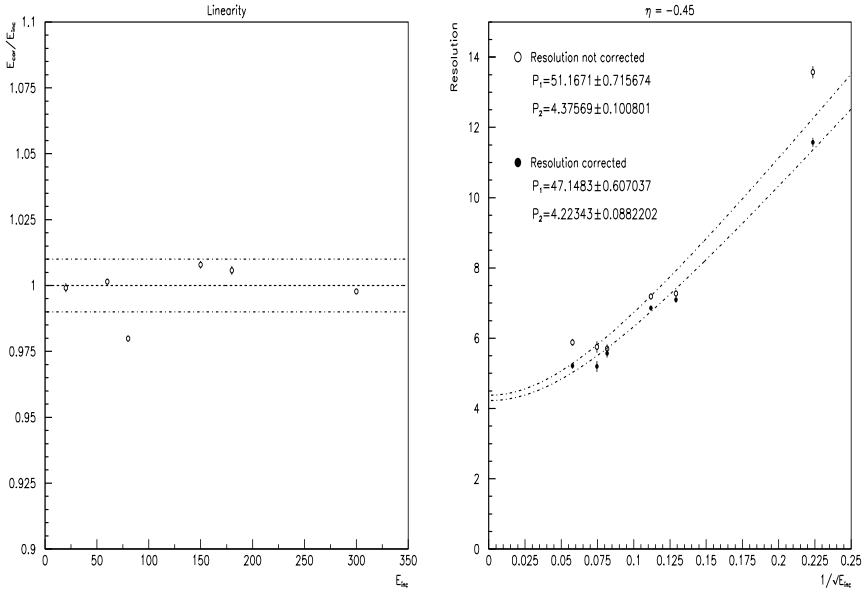

Figure 15: Linearity and resolution of reconstructed energy for global fit, η = -0.45, the 1996 test beam data

E_{inc}	$\eta_{notcorr}$	$\eta^{(1)}_{corr}$	P_1	α
20.	12.98 ± 0.16	12.76 ± 0.15	0.780 ± 0.020	7.550 ± 6.953
60.	8.37 ± 0.12	8.10 ± 0.11	0.779 ± 0.030	5.479 ± 3.200
80.	8.16 ± 0.09	7.72 ± 0.08	0.761 ± 0.024	5.087 ± 2.106
150.	6.90 ± 0.13	6.30 ± 0.11	0.759 ± 0.057	3.816 ± 2.729
150.	7.22 ± 0.20	6.07 ± 0.15	0.768 ± 0.081	3.543 ± 3.314
180.	6.57 ± 0.11	5.89 ± 0.09	0.755 ± 0.059	3.192 ± 2.060
300.	6.83 ± 0.16	5.69 ± 0.11	0.735 ± 0.101	2.437 ± 1.966

Table 2: Comparison of corrected and not corrected resolution, $\eta = -0.25$, the 1996 test beam data, standalone fit.

E_{inc}	$\eta_{notcorr}$	$\eta^{(1)}_{corr}$	α
20.	12.98 ± 0.16	12.87 ± 0.15	5.467 ± 2.090
60.	8.37 ± 0.12	8.06 ± 0.11	4.281 ± 1.488
80.	8.16 ± 0.09	7.74 ± 0.08	5.230 ± 1.390
150.	6.90 ± 0.13	6.32 ± 0.11	3.993 ± 1.413
150.	7.22 ± 0.20	6.26 ± 0.16	3.340 ± 1.537
180.	6.57 ± 0.11	5.89 ± 0.10	3.495 ± 1.006
300.	6.83 ± 0.16	5.67 ± 0.12	3.092 ± 0.922

Table 3: Comparison of corrected and not corrected resolution, $\eta = -0.25$, the 1996 test beam data, fit with $P_1 = 0.762$.

E_{inc}	$\eta_{notcorr}$	$\eta^{(1)}_{corr}$
20.	12.98 ± 0.16	12.83 ± 0.15
60.	8.37 ± 0.12	8.17 ± 0.11
80.	8.16 ± 0.09	7.69 ± 0.08
150.	6.90 ± 0.13	6.35 ± 0.12
150.	7.22 ± 0.20	6.31 ± 0.17
180.	6.57 ± 0.11	5.91 ± 0.10
300.	6.83 ± 0.16	5.70 ± 0.12

Table 4: Comparison of corrected and not corrected resolution, $\eta = -0.25$, the 1996 test beam data, global fit with $P_1 = 0.762$, $\alpha = \exp(1.679 - 0.2054 \cdot 10^{-2} \cdot E_{inc})$

E_{inc}	$\eta_{notcorr}$	$\eta^{(1)}_{corr}$	P_1	α
20.	13.57 ± 0.17	11.74 ± 0.13	0.762 ± 0.018	6.418 ± 3.526
60.	7.27 ± 0.09	7.09 ± 0.08	0.762 ± 0.020	4.756 ± 2.740
80.	7.19 ± 0.07	6.90 ± 0.06	0.747 ± 0.015	4.858 ± 2.198
150.	5.71 ± 0.12	5.54 ± 0.12	0.769 ± 0.035	3.907 ± 5.920
180.	5.75 ± 0.17	5.15 ± 0.15	0.761 ± 0.048	3.159 ± 5.580
300.	5.88 ± 0.10	5.22 ± 0.09	0.763 ± 0.027	2.764 ± 1.761

Table 5: Comparison of corrected and not corrected resolution, $\eta = -0.45$, the 1996 test beam data, standalone fit.

E_{inc}	$\eta_{notcorr}$	$\eta^{(1)}_{corr}$	α
20.	13.57 ± 0.17	11.63 ± 0.13	6.479 ± 3.182
60.	7.27 ± 0.09	7.05 ± 0.08	4.853 ± 2.360
80.	7.19 ± 0.07	6.93 ± 0.07	6.683 ± 3.383
150.	5.71 ± 0.12	5.65 ± 0.12	3.465 ± 2.471
180.	5.75 ± 0.17	5.21 ± 0.17	3.270 ± 2.807
300.	5.88 ± 0.10	5.22 ± 0.08	2.749 ± 1.260

Table 6: Comparison of corrected and not corrected resolution, $\eta = -0.45$, the 1996 test beam data, fit with $P_1 = 0.762$.

E_{inc}	$\eta_{notcorr}$	$\eta^{(1)}_{corr}$
20.	13.57 ± 0.17	11.58 ± 0.13
60.	7.27 ± 0.09	7.10 ± 0.08
80.	7.19 ± 0.07	6.86 ± 0.06
150.	5.71 ± 0.12	5.57 ± 0.12
180.	5.75 ± 0.17	5.19 ± 0.15
300.	5.88 ± 0.10	5.22 ± 0.09

Table 7: Comparison of corrected and not corrected resolution, $\eta = -0.45$, the 1996 test beam data, global fit with $P_1 = 0.762$. $\alpha = \exp(1.871 - 0.3061 \cdot 10^{-2} \cdot E_{inc})$